  Bull. Chem. Soc. Jpn., 56, 379—385 (1983)

A Study of Local Structure Formation in Binary Solutions of 2-Butoxyethanol and Water by Rayleigh Scatterring and Raman Spectra

Nobuyuki Ito,† (the late)Tsunetake Fujiyama, and Yasuo Udagawa*

Institute for Molecular Science, Myodaiji, Okazaki 444

†*Department of Chemistry, Faculty of Science, Tokyo Metropolitan University, Setagaya-ku, Tokyo 158*

(Received June 22, 1982)

The concentration dependence of concentration fluctuations at 21, 32, and 42 °C and of Raman spectra at 21 °C were measured for binary solutions of 2-butoxyethanol (BE) and water. The existence of the two kinds of local structures is inferred; clathrate hydrate-like structure $g[(H_2O)_{50}BE]$ and aggregate $h[(H_2O)_4BE]$. The compositions of these two structures are the same as those of the two phases into which the solution separates above the critical solution temperature. The phase separation is understood to be the end of the growth of the local structures, which already exist well below the critical solution temperature.

Molecules such as acetone and *t*-butyl alcohol (TBA) are known to form solid clathrate hydrates at low temperature.[1] The existence of clathrate hydrate-like structure of these molecules has been reported in aqueous solutions also.[2-5] In the binary solution of TBA and water, an increase in the mean-square concentration fluctuations with temperature has been observed and interpreted to be due to the growth of clathrate hydrate-like structure. This has lead us to conjecture that the growth of the aggregates with temperature eventually causes phase separation.[2] Since the TBA–water mixture does not show phase separation at atmospheric pressure, however, the relationship between the local structure formation and the phase separation has not been proved.

The binary solution of 2-butoxyethanol (BE) and water is known to show phase separation and has a lower critical solution temperature (LCST) at atmospheric pressure. In the previous work the concentration fluctuation and mutual diffusion coefficients at 21 °C were reported and the formation of clathrate hydrate-like structure was concluded.[4] In the present work, concentration fluctuations are measured at various temperatures below the LCST in order to make clear the relationship between the local structure formation and the phase separation.

The formation of local structures in BE–water mixture has been postulated because of thermodynamic studies[9] and light scattering measurements,[4] but it seems that no one has studied it in terms of molecular structure. In the formation of clathrate hydrate-like structure, flexible molecules such as BE with many internal rotational axes are expected to show conformational changes. In other words, observation of conformational changes would be evidence for such a structure. Vibrational spectroscopy is known to be sensitive to such changes. In this paper Raman spectra of BE at various concentration are investigated in relation to the conformational changes by local structure formation.

Experimental

Measurements of Concentration Fluctuations. The light scattering spectra were observed with a spectrometer designed and constructed in our laboratory.[5] The refractive indices of the sample solution were measured by means of an Abbe refractometer (Atago). All the measurements were performed at 21, 32, and 42 °C (±0.5 °C).

Measurements of Raman Spectra. The Raman spectra were obtained at 21 °C by the use of a Spex 1403 spectrometer with a Spectra Physics 165-09 argon ion laser.

Measurement of Miscibility Curve. The miscibility curve was measured by the following procedures. The samples in sealed tubes were set in a water bath and irradiated with a He–Ne laser light. By the visual observation of scattered light with raising the temperature, the phase-separation temperatures were determined. Each point recorded is the average of at least two readings. The temperature was measured by the use of a Hewlett Packard quartz thermometer (model 2804A).

Materials. 2-Butoxyethanol (BE) purchased from Tokyo Kasei Co. Ltd. was used without further purification for the measurements of light scattering and Raman spectra. BE used for the measurement of the miscibility curve was, distilled with a spinning band distiller. The purity was ascertained to be better than 99.99% by gas chromatography. Water was passed through the Mili-Q Purification System (Millipore) after distillation. The relative electric resistance of water was more than 15 MΩ cm^{-1}. Deuterium oxide purchased from E. Merck AG. was used for the measurement of Raman Spectra without further purification.

Normal Coordinate Calculations. For the assignments of Raman bands, a normal coordinate treatment was carried out with a computer program NCTB (IMS program library) and HITAC M 200Hcomputer system at the Computer Center of Institute for Molecular Science (IMS).

Results

Concentration Fluctuations and the Miscibility Curve. Figure 1 shows the miscibility curve obtained in this work along with those reported in the literatures.[6,7] It was noticed that the miscibility curve is strongly affected by the existence of impurities. This is the reason for the wide discrepancies in the literature. Accordingly special care was taken to purify the material and the curve reported here is believed to be better than those previously reported. BE and water mix at all temperatures in the concentration range of $x_{BE}<0.02$ and $x_{BE}>0.2$, but the solution separates into two phases upon raising the temperature when $0.02<x_{BE}<0.2$. The steep edges of the miscibility curve at both ends suggest that the concentrations of the two phases have tendencies to be close to 0.2 or 0.02. This implies that the solution have particularly stable structures when $x_{BE}=0.02$ an 0.2. It is found that the LCST is 49.4 °C

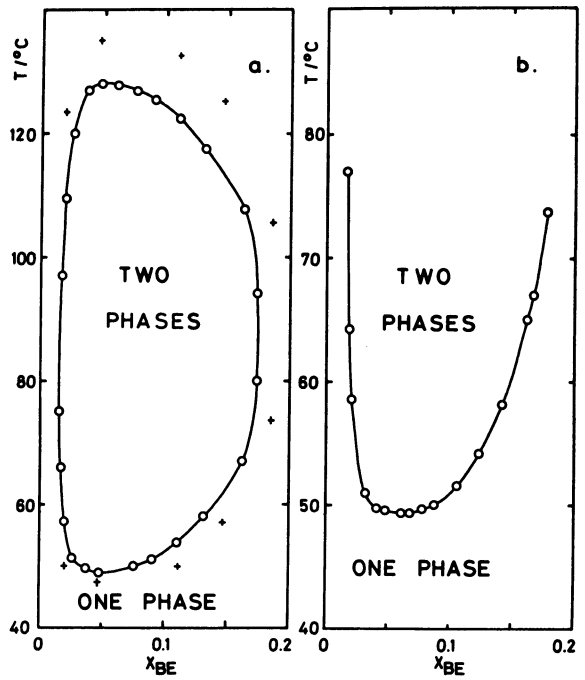

Fig. 1. Miscibility curves of 2-butoxyethanol and water mixture.
(a): ○ is from Ref. 6 and + is from Ref. 7, (b): present results.

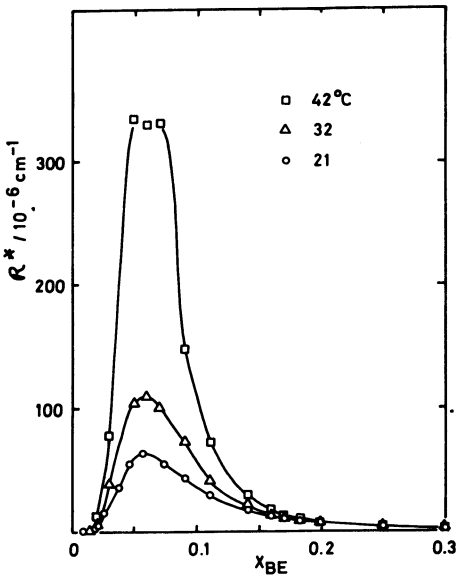

Fig. 2. Concentration dependence of Rayleigh intensities for BE–water mixtures.

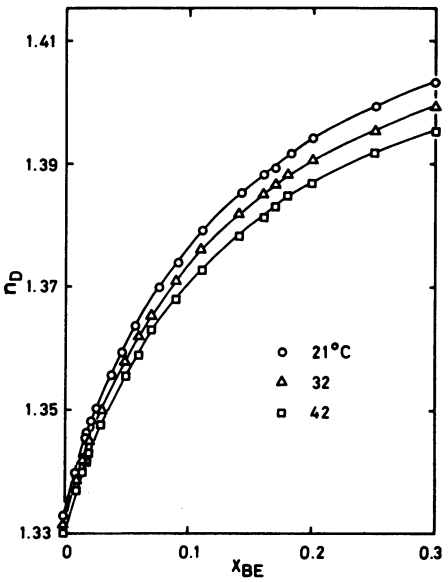

Fig. 3. Concentration dependence of the refractive index of BE–water mixtures.

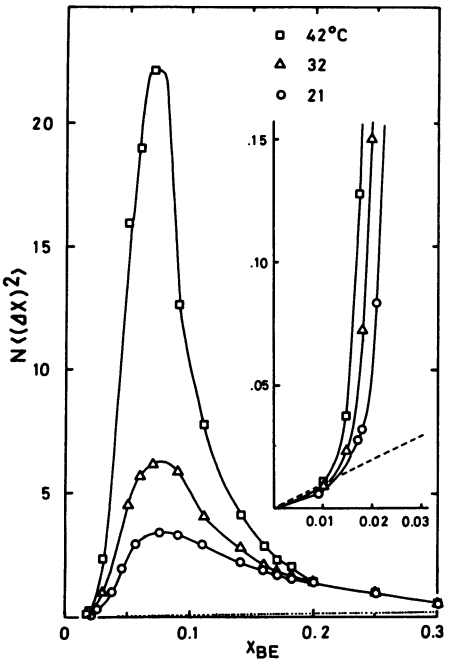

Fig. 4. Concentration dependence of the concentration fluctuation observed for BE–water mixtures. The dashed line corresponds to the concentration fluctuation expected for a n ideal binary solution.

at $x_{BE}=0.07$. As will be shown below the concentration fluctuations $N\langle(\Delta x)^2\rangle$ take its maximum value at the same concentration as the LCST. This indicates that local structure formation is closely related to the phase separation.

The concentration fluctuations can be derived from the light scattering intensity and the refractive indices which are shown in Figs. 2 and 3, respectively. The procedure is the same as described in the previous paper.[8] The isobaric heat capacity and the density necessary for the calculation were obtained from the literature.[9] In Fig. 4 the mean-square concentration fluctuations, $N\langle(\Delta x)^2\rangle$, at various temperatures are plotted against the mole fraction of BE, x_{BE}, where N is the total number of molecules in the observation volume. The dashed line in the figure corresponds to the $N\langle(\Delta x)^2\rangle$ expected for an ideal binary solution. It is seen from the figure that the observed concentration fluctuations are close to those of an ideal binary solution in the concentration range $0<x_{BE}<0.02$. However, it increases abruptly near $x_{BE}=0.02$, attains a maximum

at about $x_{BE}=0.07$, the value of which is about two orders of magnitude larger than that of the ideal solution, and decreases gradually with the increase of concentration of BE, and especially above 0.2 it varies little in magnitude. Also it is noticed from the figure that the $N<(\Delta x)^2>$ increases rapidly with temperature in the concentration range $0.02<x_{BE}<0.2$. On the other hand, it is almost independent of the temperature if x_{BE} is above 0.2 and below 0.02.

Analysis of $N<(\Delta x)^2>$. In the previous papers we have reported that the local structures existing in the solution can be determined from the analysis of the concentration dependence of $N<(\Delta x)^2>$.[8] In the case of the ideal solution the concentration fluctuation is expressed as $x_B(1-x_B)$ for the binary solution of A and B, where x_B is the mole fraction of B. In the case where the same species gather together, the concentration fluctuation is greater than that of the ideal solution. In the case in which the different species gather together, the concentration fluctuation is smaller than that of the ideal solution. The observed concentration fluctuation indicates that BE-water mixture belongs to the former case.

From a comparison of the concentration dependence of $N<(\Delta x)^2>$ with the miscibility curve, we can make a picture of the local structure formed in the solution. It is seen from Fig. 1 and Fig. 4 that the concentration where the concentration fluctuations increase/decrease corresponds to that where the miscibillity curve rises/falls. As mentioned above, this suggests the fact that stable local structures are formed at these concentrations. Their compositions must be $A_{50}B$ and A_4B, where A means water and B means BE, because the concentrations at issue are 0.02 and 0.2.

In order to understand the mixing state of BE-water mixture in all the concentration range, the following model is assumed; (1) local structures of types A_l and A_lB ($l=50$) in the concentration range $0<x_B<0.02$, (2) simultaneous existence of A_lB and A_mB ($l=50$, $m=4$) in the concentration range $0.02<x_B<0.2$, and (3) a local structure of type A_mB ($m=4$) and molecules B in the concentration range $0.2<x_B$. The distribution of the two types of local structure calculated from the model above is shown in Fig. 5a. The concentration fluctuation for this model can be calculated for the following concentration range as:

$$[0<x_B<0\ 02]$$
$$N\langle(\Delta x_B)^2\rangle = x_B(1-x_B)[1-(l+1)x_B] \quad (2a)$$
$$[0\ 02<x_B<0\ 2]$$
$$N\langle(\Delta x_B)^2\rangle = x_B[(l+1)x_B-1][1-(m+1)x_B] \quad (2b)$$
$$[0\ 2<x_B<0\ 3]$$
$$N\langle(\Delta x_B)^2\rangle = x_B(1-x_B)[1-(m+1)x_B] \quad (2c)$$

Figure 5b demonstrates the concentration dependence of concentration fluctuations calculated from Eq. 2 for $l=50$ and $m=4$. The calculated concentration fluctuations coincide well with the observed ones in the following ways: (1) The calculated concentration fluctuation is small and close to that expected for the ideal solution for $0<x_B<0.02$, and (2) it has a minimum at near $x_{BE}=0.02$ and 0.2 where the slope of observed ones change abruptly, and (3) it reaches a maximum in the concentration rage of $0.02<x_B<0.2$.

However, the observed concentration fluctuation is much greater than the calculated one by an order of magnitude, as is noticed from the ordinate of Fig. 4 and Fig. 5b. In order to overcome this, we have to modify the model in the following manner. In the concentration range of $0.02<x_B<0.2$, the local structures of types A_lB and A_mB gather together and form $g(A_lB)$ and $h(A_mB)$, respectively. In this case the concentration fluctuation is given by the following equation:

$$N\langle(\Delta x_B)^2\rangle=(l-m)^{-1}[(l+1)x_B-1][1-(m+1)x_B] \times\{g[(l+1)x_B-1]+h[1-(m+1)x_B]\} \quad (2b')$$

The concentration fluctuations increase with both g and h, but these two can not be determined independently.

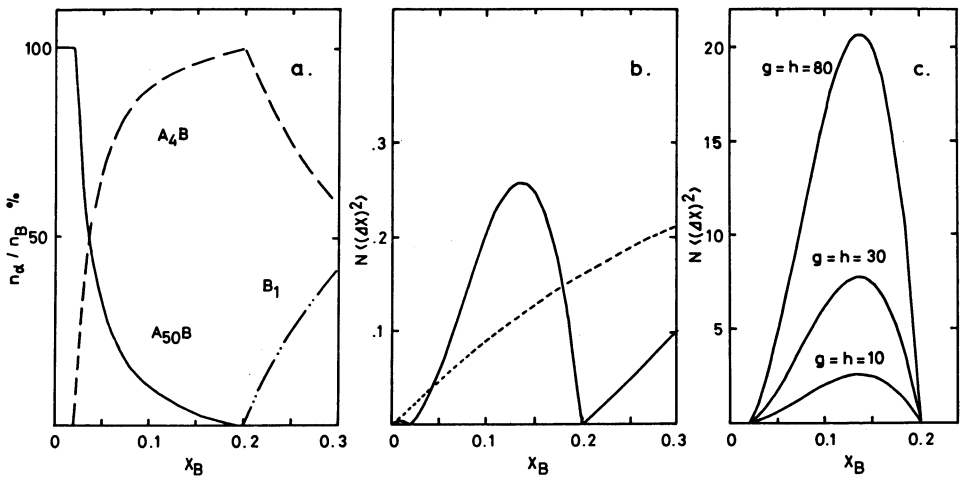

Fig. 5. (a) Distribution of B molecules among several local structures α; $A_{50}B$, A_4B, and B_1. In the figure n_B means the total number of B molecule and n_α means the number of α species. All the B molecules are in $A_{50}B$ for $0<x_{BE}<0.02$, in $A_{50}B$ and A_4B for $0.02<x_{BE}<0.2$, and in A_4B and B_1 for $0.2<x_{BE}<0.3$. (b) The theoretical value of concentration fluctuation calculated from Eq. 2. (c) The theoretical value calculated from Eq. 2b′ in the concentration range $0.02<x_{BE}<0.2$ for $g=h=10$, 30, and 80.

By arbitrarily assuming $g=h$, the calculated concentration fluctuations are shown in Fig. 5c. The maximum values of observed ones at 21 and 42 °C are close to calculated ones when $g=h$ are about ten and one hundred, respectively. Also it takes maximum at about $x_B=0.1$ in both the observed and calculated ones.

While the calculated concentration fluctuation become zero at $x_B=0.02$ and 0.2, the observed one does not. In the above model, all the local structure is assumed to be $A_{50}B$ and A_4B at 0.02 and 0.2, respectively. This is improved by taking the following association equilibrium Eq. 3 into consideration. Although the association of A_{50} may proceed stepwise in real solution, Eq. 3 is assumed since this is the simplest form in order to examine the contribution of the equilibrium. If more equilibrium were taken into account, the calculation should be tedious and meaningless for the understanding of the mixing state of binary solution.

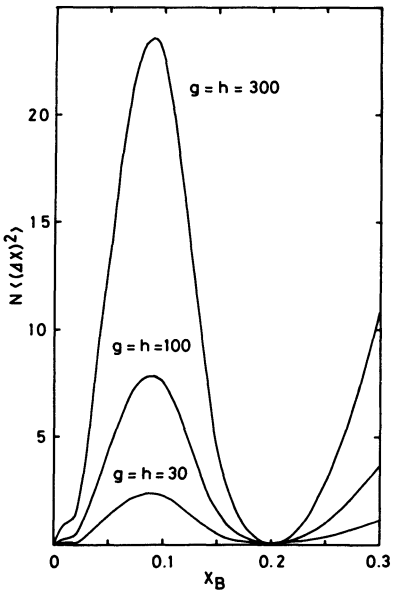

Fig. 6. Theoretical value of concentration fluctuation calculated by equillibrium of Eq. 3 for $g=h=30$, 100, 300, $K_1=10^3$, $K_2=10$, and $K_3=1$.

$$A_{50} + B \rightleftharpoons K_1 \rightleftharpoons A_{50}B \longrightarrow g(A_{50}B) \quad (3a)$$

$$A_4 + B \rightleftharpoons K_2 \rightleftharpoons A_4B \longrightarrow h(A_4B) \quad (3b)$$

$$4A_{50} \rightleftharpoons K_3 \rightleftharpoons 50A_4 \quad (3c)$$

Figure 6 shows the concentration dependence of concentration fluctuation numerically calculated assuming the above equilibrium for $K_1=10^3$, $K_2=10$, $K_3=1$, and various $g=h$. The calculated concentration fluctuations correspond more closely with the observed ones. Figure 7 shows the aggregation schematically. In principle it is possible to search for the best set of parameters (K_1, K_2, K_3, l, m, g, h) that gives the best fit to the observed concentration fluctuation. This was not attempted because none of them can be determined uniquely.

From the analysis of concentration fluctuation given above the following conclusions are obtained. (1) For $0<x_{BE}<0.02$ local structures of types $A_{50}B$ and A_{50} are formed. (2) For $0.02<x_{BE}<0.2$ local structures of types $g(A_{50}B)$ and $h(A_4B)$ exist simultaneously. The values of g and h depend on temperature, and vary between ten and several hundreds. (3) For $0.2<x_{BE}$ the local structures of types $h'(A_4B)$ and B_1 are formed, where the value of h' is independent of temperature. The conclusions are consistent with the Raman Spectra described in the following section.

Raman Spectra. Raman spectra of aqueous BE solution at various concentrations were obtained in order to ascertain whether a conformational change of BE occurs through the formation of clathrate hydrate-like structure. Shimanouchi *et al.* studied the Raman and IR spectra of many long chain ethers and have reached the following conclusions.[10] (1) Various rotational isomers due to many internal rotation axes exist in the liquid state. (2) The spectra of the various isomers are different, especially in the 200—600 cm^{-1} region of the skeletal deformation and torsional vibration modes and in the 800—1200 cm^{-1} region of the skeletal stretching and methyl and methylene rocking vibrations. Since the conformation of BE molecule is supposed to alter when it is within a clathrate hydrate structure, the change of the Raman spectra in these two regions are expected. Since water has a strong and broad Raman signal in the low frequency region, however, only the high frequency region gave positive results.

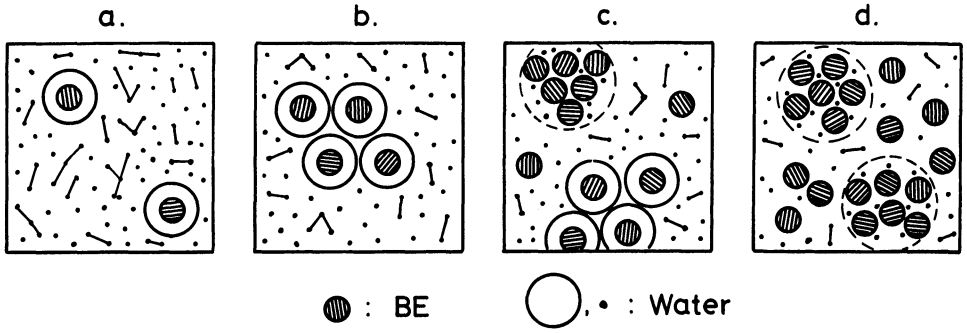

Fig. 7. Mixing state of BE–water mixtures drawn schematically. (a); for $0.02>x_{BE}$, (b); for $0.02<x_{BE}<0.05$, (c); for $0.05<x_{BE}0.2$, and (d); for $0.2<x_{BE}$. (○, ●) and ◍ correspond to the water molecule and the BE molecule, respectively. ◎ and ❁ mean clathrate hydrate-like structure $g(A_{50}B)$ and aggregate $h(A_4B)$, respectively.

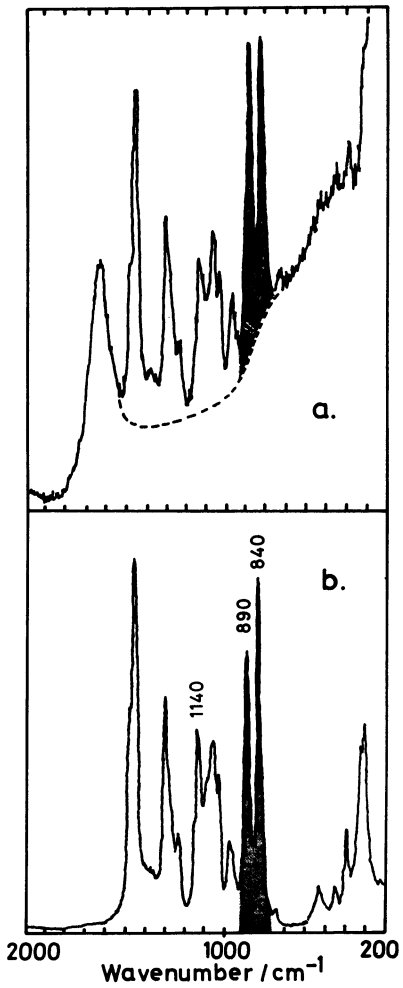

Fig. 8. Observed Raman spectra of aqueous BE solution of x_{BE}=0.009 (a) and neat liquid of BE (b) in the 200—2000 cm^{-1} region. Dashed line in (a) is the scattering from solvent water.

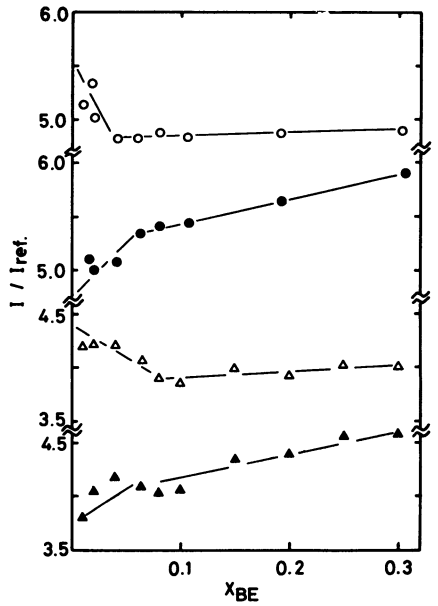

Fig. 9. Intensities of 840 and 890 cm^{-1} peaks relative to the intensity of 970 cm^{-1} peak in the Raman spectra of BE as functions of the concentration in aqueous solution at 21 °C. ●; $I(\approx840)/I(\approx970)$, ○;$(\approx890)/I(\approx970)$. For BE–deuterium oxide mixture, ▲; $I(840)/I(\approx970)$, △; $I(\approx890)/I(\approx970)$.

In Fig. 8 the Raman spectra of neat liquid and aqueous (x_{BE}=0.009) solution of BE are shown. From the comparison of Fig. 8a and b, it is evident that the peak intensities of bands at 840, 890, and 1140 cm^{-1} change with the concentration of BE. Out of the above three bands the one at 1140 cm^{-1} shifts in the BE–deuterium oxide solution, and is due to alcoholic OH groups. By comparison with Shimanouchi *et al.*'s results, the other two can be assigned to C–O stretching vibrations of ether bond. Since the bandwidths scarcely alter with concentration, peak heights can be taken as intensities if background from the solvent is properly subtracted. Figure 9 shows the intensity ratios of the 840 and 890 cm^{-1} bands to the 970 cm^{-1} band as a function of concentration.[11] As is seen from the dotted line in Fig. 8, a broad Raman signal from the solvent water overlaps the BE Raman signal and may lead to error. Since the use of deuterium oxide reduces the overlap, the data with deuterium oxide are also obtained and shown in Fig. 9. Both water and deuterium oxide give similar results. It can be seen from Fig. 9 that the intensity of 840 cm^{-1} band decreases and that of 890 cm^{-1} band increases with concentration. However, the changes are not monotonic but rather there are bends around x_{BE}=0.05, where the change in concentration fluctuation is the largest.

These observations as well as the results of Shimanouchi *et al.* lead to the following conclusions; a clathrate hydrate-like structure is formed at low concentration and the BE molecule changes its conformation when freed from clathrate above x_{BE}=0.05. At higher concentration where x_{BE}>0.05, the conformation of BE molecules is the same as that in neat liquid. The BE molecule in clathrate must prefer a compact form to an elongated one, and must assume the gauche form around some internal rotation axes. In order to make this conclusion clearer, a normal coordinate calculation was carried out with general force constants given by Shimanouchi *et al.*[12] Unfortunately the force constants for the alcohol were not available, so the calculation was done for butyl ethyl ether. The Raman spectrum of this molecule is similar to that of BE, reflecting that the skeleton of these two are the same.

Since butyl ether has four internal rotation axes, there are thirty four rotational isomers. Shimanouchi *et al.* have reported that ethyl propyl ether (CH_3CH_2–CH_2–O–CH_2CH_3) assumes the forms of GTT and TTT, and butyl methyl ether (CH_3CH_2–CH_2–CH_2–OCH_3) takes the forms of TTT and TGT in the liquid state.[13] That is, the trans conformation about CO–CC axis is much more stable than the gauche, but gauche conformation is also as stable as the trans about C–C axis. From these results the forms of TTTT, TGTT, GGTT, and GTTT are most likely for butyl ethyl ether (CH_3CH_2–CH_2–CH_2–O–CH_2CH_3) in the liquid state. As mentioned above, the COC symmetric vibration dominates in the 800—1000 cm^{-1} region of the Raman

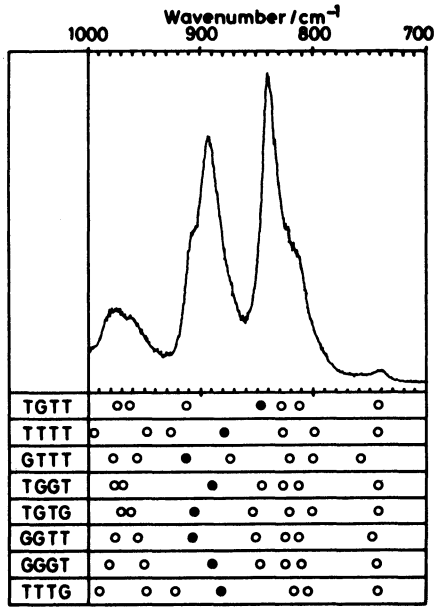

Fig. 10. Observed Raman spectra of BE and the calculated frequencies of butyl ethyl ether in the 700—1000 cm^{-1} region. Solid circles indicate C–O stretching vibrations, which are expected to dominate in this region.

spectrum of ethers,[14] and the bands at 840 and 890 cm^{-1} in Fig. 9 are assigned to this vibration of several rotational isomers. Calculations show that only TGTT has COC stretching frequency smaller than 850 cm^{-1}, and frequencies of other conformers all fall between 880 and 910 cm^{-1}, as is shown in Fig. 10. Since the intensity of 840 cm^{-1} vibration is higher than that of 890 cm^{-1}, the major form of BE is TGTT in the neat liquid. In higher concentrations of water, the intensity of 890 cm^{-1} band increases and that of the 840 cm^{-1} band decreases. This means that proportion of TGTT gets smaller with dilution and conformers such as GTTT and GGTT increase in number. By the formation of clathrate hydrate-like structure, BE is surrounded by water. Since the gauche conformation about CO–CC axis is more advantageous for the ether –O– in contact with water molecule, the conformers such as TGGT and TGTG must also increase. Nevertheless the frequency differences are too small to distinguish those rotational isomers.

Discussion

In the previous papers,[2] it was shown that in a binary solution of TBA and water the local structures of types $g[(H_2O)_{20}TBA]$ and $(H_2O)_{20}$ are formed for $0<x_{TBA}<0.04$ and local structures of types $g[(H_2O)_{20}$-TBA] and $(TBA)_s$ are formed for $0.04<x_{TBA}$. The local structure of $g[(H_2O)_{20}TBA]$ has been postulated to be a clathrate hydrate-like structure. From the analysis of mutual diffusion coefficients the clathrate hydrate-like structure has been considered to be an "aggregated polyhedron" (that is, one in which the polyhedra gather together to form an aggregate without sharing faces with each other), not an "associated polyhedron" (that is, one in which water molecules form polyhedra, each of which encages a guest molecule and that the several polyhedra share one of their faces).

In the binary solution of BE and water, the local structure of type $g[(H_2O)_{50}BE]$ is also considered to be "aggregated polyhedron." Below the concentration $x_{BE}=0.05$ more BE molecules whose conformation is close to spherical one are expected to exist from the analysis of Raman spectra. The conformation change of BE must be due to the formation of polyhedra of water molecules. The difference in size between the polyhedra formed in TBA–water and those in the BE–water mixture arises from the difference in bulk of the hydrophobic group of the two molecules. Above the concentration $x_{BE}=0.05$, the local structure of type $g[(H_2O)_{50}$-BE] is destroyed and the amount of local structures of type $h[(H_2O)_4BE]$ increases due to the increase of BE molecules, as shown in Fig. 8a, where the distribution of two types of local structures is expressed as $A_{50}B$ and A_4B, respectively. Formation of the local structure of type $h[(H_2O)_4BE]$ is reminiscent of micelles in an aqueous solution of surfactants. BE molecule is a member of polyethylene glycol monoalkyl ether $C_nH_{2n+1}O(CH_2CH_2O)_mH$ family where $n=4$ and $m=1$. Micelle formation is known in this class of molecules where $n\geqq 8$ in the case of $m=1$. The critical micelle concentration (CMC) for $n=8$ and $m=1$ is 4.9 mmol/l (that is, about 1×10^{-4} in the mole fraction of solute) which is about five hundred times lower than the concentration at which BE takes the form $h[(H_2O)_4BE]$. Since BE has a relatively strong affinity for water, the hydrophobic interaction between BE molecules is weaker than that between its longer chain homologs. It does not have distinct CMC.

The phase transition is understood from the idea of the local structure in the following manner. The increase of concentration fluctuation with temperature is caused by the increase of either g and h of local structures of types $g[(H_2O)_{50}BE]$ and $h[(H_2O)_4BE]$. That is, by raising the temperature the "aggregated polyhedron" and the aggregates of BE molecules gather together and become larger, and finally the solution separates into two phases at critical solution temperature. Therefore the phase separation is the result of the growth of local structures which already exist about thirty degrees below the LCST. In TBA–water mixture the aggregate of TBA does not seem to become large enough with the increase of temperature. This can be attributed to the small size of hydrophobic part of TBA.

The existence of local structure has been postulated by a thermodynamic study of G. Roux, G. Perron, and J. E. Desnoyers. They have reported the apparent molal heat capacity ϕ_c and volume ϕ_v.[9] They indicate that the change in mixing states occurs near the concentration $x_{BE}=0.02$ where ϕ_c has maximum, and the microphase which is constructed from aggregate of BE is made beyond the concentration. They have also pointed out that the clathrate hydrate-like structures may be formed in the concentration region where ϕ_c has a maximum. The present results support their explanation from another viewpoint.

Concluding Remark. The phase separation phe-

nomenon has been treated as one of the critical phenomena which occur at near critical solution temperature. The present results indicate that the phase separation occurs in microscopic regions even thirty degrees below the critical solution temperature. It is well-known that there is an LCST in many nonelectrolyte aqueous solutions. The formation of local structures with clathrate hydrate-like structure and the aggregates of solutes will be common in those systems and essential factors for phase separation.

The authors wish to express their thanks to Dr. Yoko Sugawara of the Institute for Physical and Chemical Research for her help in the normal coordinate calculation with a computer program LCTB. We also would like to thank Prof. J. E. Desnoyers of Univ. de Sherbrooke for suggesting to us this interesting system, Prof. Hidemasa Takaya of IMS for his helpful advices for preparing high quality BE, and Prof. P. G. Wolynes of Univ. of Illinois for a critical reading of manuscript.

References

1) D. W. Davidson, "Water," ed by F. Franks, Plenum Press, New York-London (1973), Vol. 2, Chap. 3.

2) K. Iwasaki and T. Fujiyama, *J. Phys. Chem.*, **83**, 463 (1979); **81**, 1908 (1977).

3) N. Ito, T. Kato, and T. Fujiyama, *Bull. Chem. Soc. Jpn.*, **54**, 2573 (1981).

4) N. Ito, K. Saito, and T. Fujiyama, *Bull. Chem. Soc. Jpn.*, **54**, 991 (1981).

5) T. Kato, M. Yudasaka, and T. Fujiyama, *Bull. Chem. Soc. Jpn.*, **54**, 1632 (1981).

6) H. L. Cox and L. H. Cretcher, *J. Am. Chem. Soc.*, **48**, 451 (1926).

7) G. Poppe, *Bull. Soc. Chim. Belg.*, **44**, 640 (1935).

8) K. Iwasaki, Y. Katayanagi, and T. Fujiyama, *Bull. Chem. Soc. Jpn.*, **49**, 2988 (1976): T. Kato, and T. Fujiyama, *J. Phys. Chem.*, **80**, 2771 (1976).

9) G. Roux, G. Perron, and J. E. Desnoyers, *J. Solution Chem.*, **7**, 639 (1978).

10) T. Shimanouchi, Y. Ogawa, M. Ohta, H. Matsuura, and I. Harada, *Bull. Chem. Soc. Jpn.*, **49**, 2999 (1976).

11) It is seen from Raman spectra that the peak intensity of 970 cm^{-1} scarcely change with the concentration. By the calculation, this band is assinged as CH_2 rocking vibration.

12) T. Shimanouchi, H. Matsuura, Y. Ogawa, and I. Harada, *J. Phys. Chem. Ref. Data*, **7**, 1323 (1978).

13) The generic symbols T and G which represent the conformation of rotational isomers is described in Ref. 10.

14) F. R. Dollish, W. G. Fateley, and F. F. Bentley, "Characteristic Raman Frequencies of Organic Compounds," John Wiley and Sons, Inc., New York (1974), Chap. 3. It has been known that the CCO symmetric vibration of alcohol is also strong in the 800—1000 cm^{-1} region. The intensity of the Raman band of ethanol at 890 cm^{-1}, however, dose not show concentration dependence. Therefore the concentration dependence of 890 cm^{-1} in BE–water mixture is due to the conformational change of butoxy group.